

# Turn up the volume – Listening to hot dark sector phase transitions.

Seminar talk at Carleton University

---

Carlo Tasillo,  
Deutsches Elektronen Synchrotron (DESY)

Based on work with Fatih Ertas and Felix Kahlhöfer  
published in [2109.06208], JCAP01(2022)???

January 17, 2022



## Outline of this talk.

- 1 Why dark sector phase transitions?
- 2 Thermal evolution of dark sectors after a phase transition
- 3 The dark photon model
- 4 Conclusions

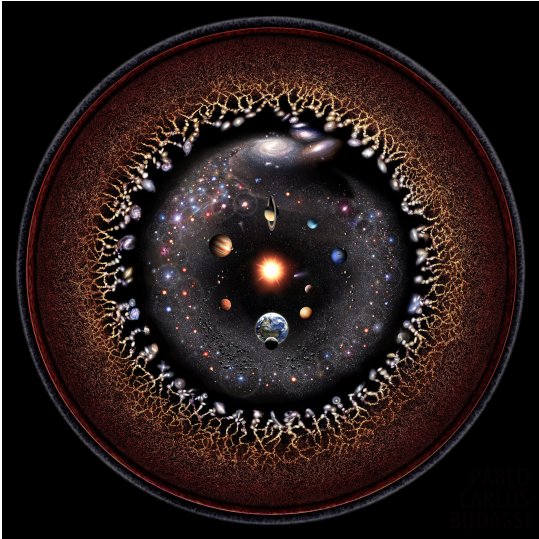


[Camille Flammarion, 1888]

## Why dark sector phase transitions?

---

# What we know about our Universe.



[Pablo Carlos Budassi, 2020]

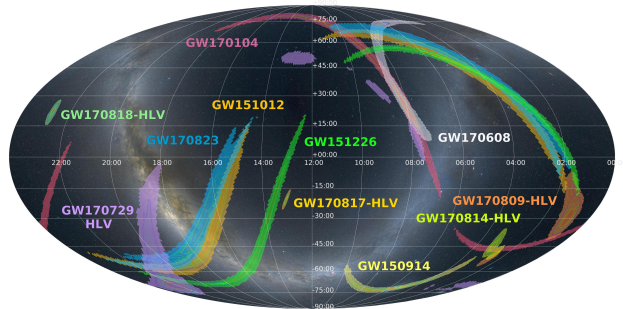
From CMB anisotropies:  $\Lambda$ CDM model

- Isotropic and homogeneous
- 13.8 billion years old
- Expands with a rate of about  $68 \text{ km s}^{-1} \text{ Mpc}^{-1}$
- 95 % of today's energy content is dark!?

👉 **What lies beyond the surface of last scattering?**

# Gravitational waves as a “new” messenger.

- Observed 90 compact binary mergers since 2015
- Sensitivity will increase considerably with start of LISA, Einstein Telescope, etc.



[LIGO, Virgo & KAGRA Collaboration, 2020]

~> **What will the stochastic gravitational wave background look like?**

## Sources of gravitational radiation: Some examples.

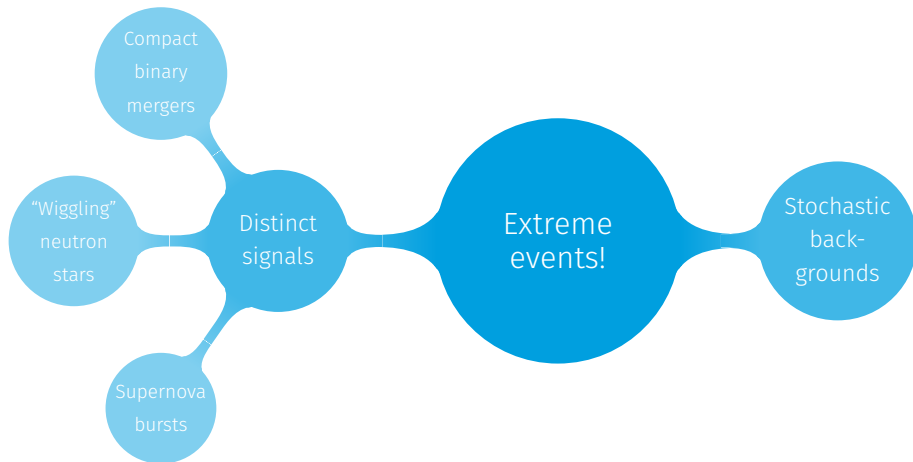


Extreme  
events!

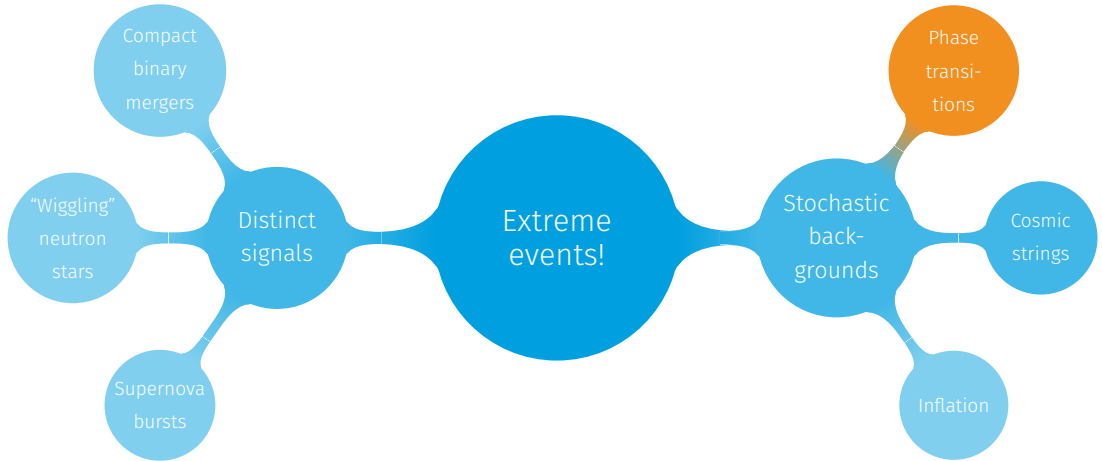
## Sources of gravitational radiation: Some examples.



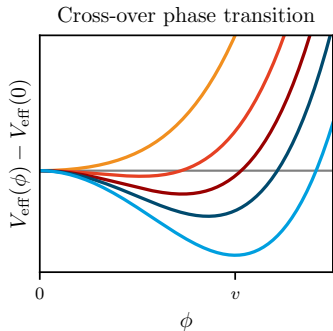
## Sources of gravitational radiation: Some examples.



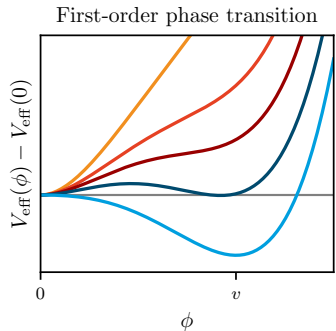
# Sources of gravitational radiation: Some examples.



## Cross-over and first-order phase transitions.



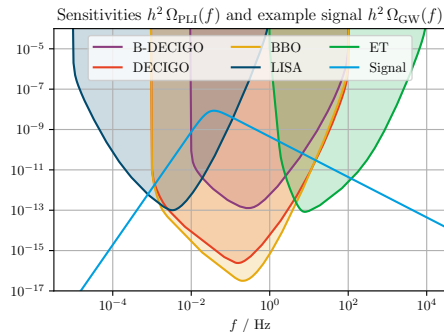
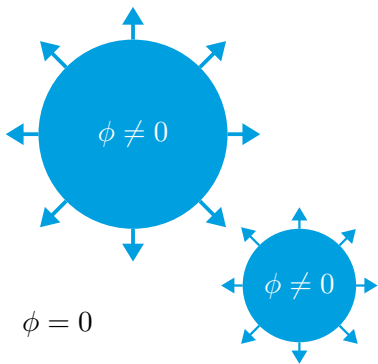
The scalar field “rolls down” from  $\phi = 0$  to  $\phi = v$ , when the bath cools from **high temperatures** to **low temperatures**.



The scalar field tunnels to the true potential minimum ( $\phi \neq 0$ ) to minimize its action ( $\sim$  free energy).

# Gravitational waves from first-order phase transitions.

Bubbles of the new phase nucleate, collide and perturb the surrounding plasma...



... giving rise to a stochastic gravitational wave background which could be observed in some years.

## Objective of this talk.

We have seen that

- Primordial GWs could be used for “listening” beyond the CMB
- First-order phase transitions emit gravitational wave signals
- Majority of our Universe is “dark”
- ↪ What kind of **dark sector** could produce observable GW signals?

**Dark sector:** particle bath without thermal contact to SM particles:

$$T_{\text{DS}} = \xi T_{\text{SM}}$$

Breitbach et al. [1811.11175] showed that **cold** ( $\xi < 1$ ) dark sectors produce weak signals...

## Objective of this talk.

We have seen that

- Primordial CMB “listening” bubble
- First-order phase transition produce gravitational waves
- Majority of dark matter candidates
- What kind of dark matter can produce observable GW signals:

Can hot ( $\xi > 1$ ) dark sector phase transitions emit observable GW signals?

What happens when the dark sector finally decays to SM particles?

death without particles:

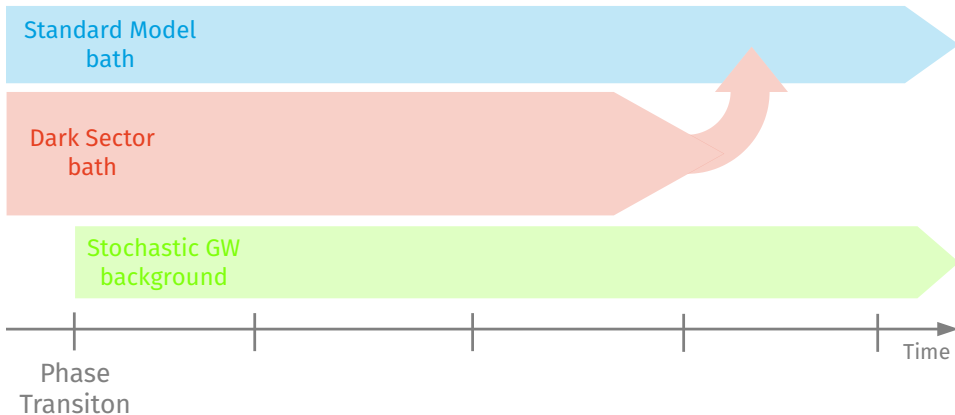
SM

[5] showed that produce weak

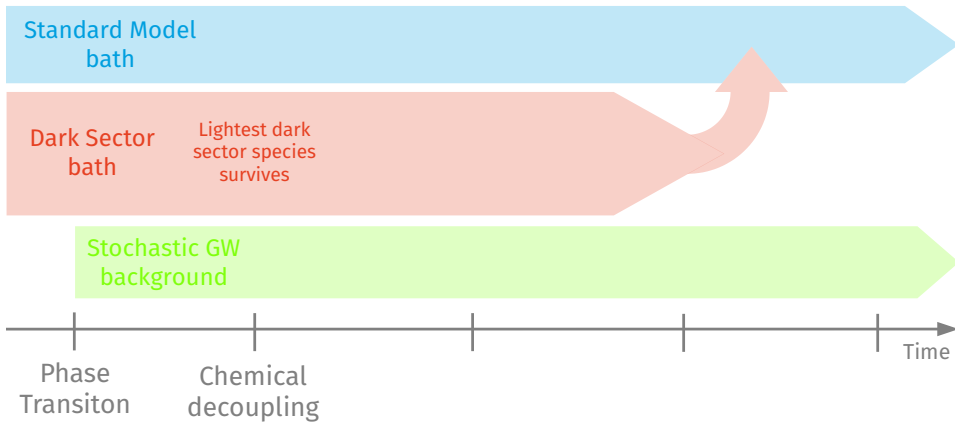
## **Thermal evolution of dark sectors after a phase transition.**

---

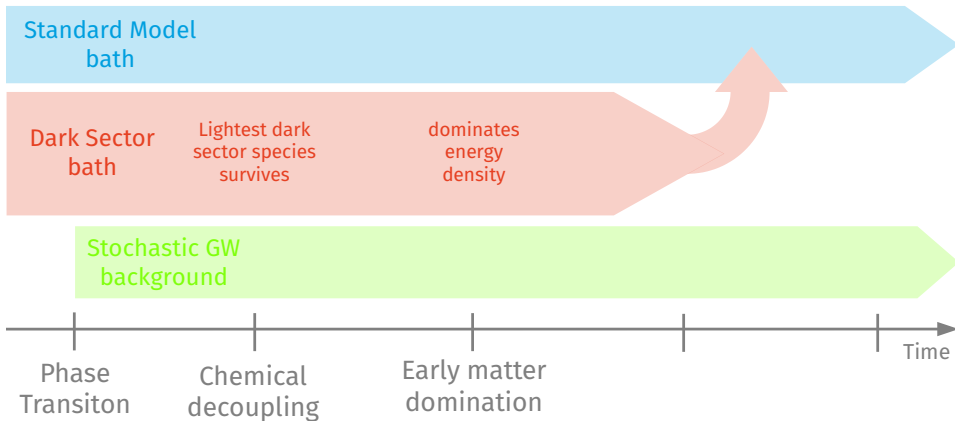
# Long-lived dark sector evolution after a phase transition.



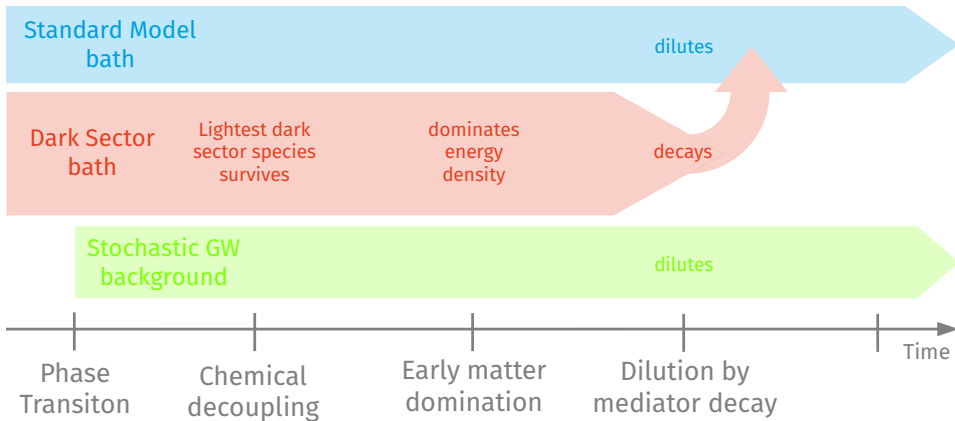
# Long-lived dark sector evolution after a phase transition.



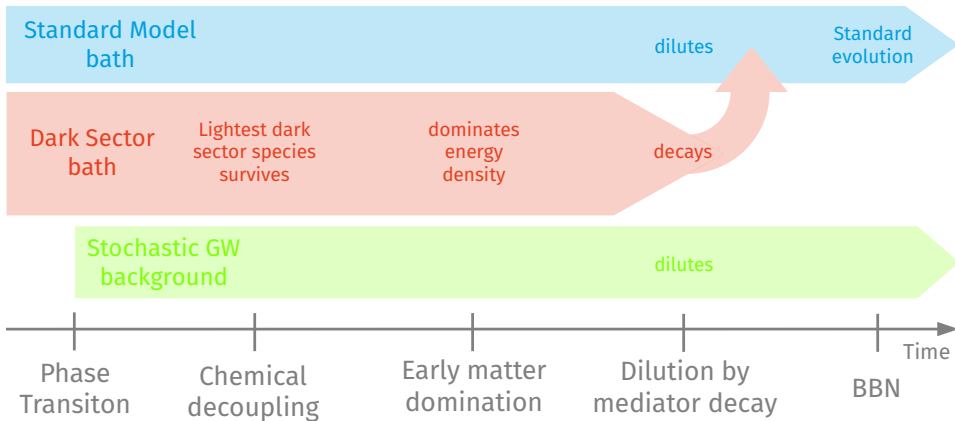
# Long-lived dark sector evolution after a phase transition.



# Long-lived dark sector evolution after a phase transition.



# Long-lived dark sector evolution after a phase transition.



## Describing the dark sector in thermal equilibrium.

For several dark sector species in thermal equilibrium: can define effective DOFs

$$\rho_{\text{tot}}(T_{\text{SM}}) = \left[ g_{\text{eff},\rho}^{\text{SM}}(T_{\text{SM}}) + g_{\text{eff},\rho}^{\text{DS}}(T_{\text{SM}}) \xi^4(T_{\text{SM}}) \right] \frac{\pi^2}{30} T_{\text{SM}}^4$$
$$s_{\text{tot}}(T_{\text{SM}}) = \left[ g_{\text{eff},s}^{\text{SM}}(T_{\text{SM}}) + g_{\text{eff},s}^{\text{DS}}(T_{\text{SM}}) \xi^3(T_{\text{SM}}) \right] \frac{2\pi^2}{45} T_{\text{SM}}^3$$

## Describing the dark sector in thermal equilibrium.

For several dark sector species in thermal equilibrium: can define effective DOFs

$$\rho_{\text{tot}}(T_{\text{SM}}) = \left[ g_{\text{eff},\rho}^{\text{SM}}(T_{\text{SM}}) + g_{\text{eff},\rho}^{\text{DS}}(T_{\text{SM}}) \xi^4(T_{\text{SM}}) \right] \frac{\pi^2}{30} T_{\text{SM}}^4$$
$$s_{\text{tot}}(T_{\text{SM}}) = \left[ g_{\text{eff},s}^{\text{SM}}(T_{\text{SM}}) + g_{\text{eff},s}^{\text{DS}}(T_{\text{SM}}) \xi^3(T_{\text{SM}}) \right] \frac{2\pi^2}{45} T_{\text{SM}}^3$$

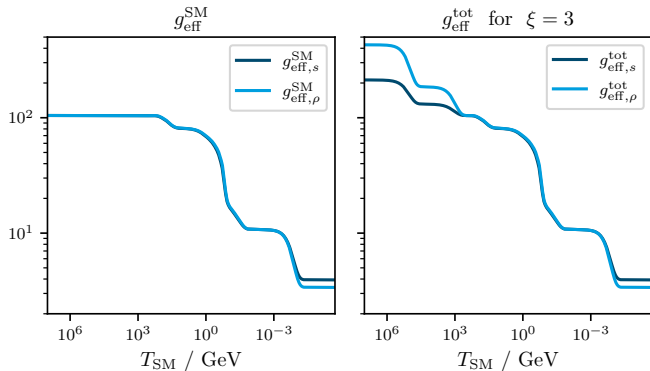
As entropy is conserved separately in the two baths, the temperature ratio follows

$$\xi(T_{\text{SM}}) = \tilde{\xi} \left( \frac{g_{\text{eff},s}^{\text{SM}}}{\tilde{g}_{\text{eff},s}^{\text{SM}}} \right)^{1/3} \left( \frac{\tilde{g}_{\text{eff},s}^{\text{DS}}}{g_{\text{eff},s}^{\text{DS}}} \right)^{1/3}$$

When SM particles annihilate  $\xi$  decreases, since the SM becomes hotter.

When dark sector DOF decrease  $\xi$  increases, since the DS becomes hotter.

## Describing the dark sector in thermal equilibrium.



**Example:** Thermal evolution of a hot ( $\xi = 3$ ) dark sector consisting of a dark photon ( $m_{\text{DP}} = 10^6$  GeV) and a dark Higgs boson ( $m_{\text{DH}} = 10^4$  GeV).

## Describing the dark sector in thermal equilibrium.



This description breaks down when the dark species no longer follow their equilibrium (Bose-Einstein) distributions.

In our setup this occurs when the lightest dark sector species has a long lifetime.

**Example:** Thermal evolution of a hot ( $\xi = 3$ ) dark sector consisting of a dark photon ( $m_{\text{DP}} = 10^6$  GeV) and a dark Higgs boson ( $m_{\text{DH}} = 10^4$  GeV).

# The out-of-equilibrium decay of a dark mediator.

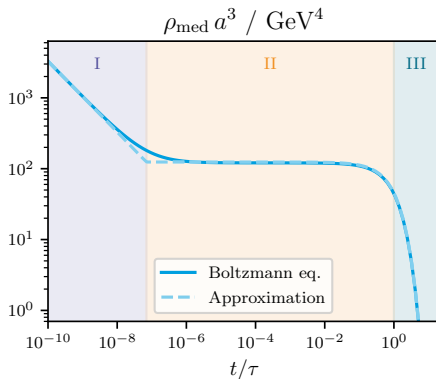
Evolution of the lightest dark sector state (“mediator”) after chemical decoupling:

$$\dot{\rho}_{\text{med}} \simeq -3 \zeta H \rho_{\text{med}} - \frac{\rho_{\text{med}}}{\tau}$$

with

$$\zeta = 1 + \frac{P_{\text{med}}}{\rho_{\text{med}}} = \begin{cases} 4/3 & \text{rel.} \\ 1 & \text{non-rel.} \end{cases}$$

Three phases: Relativistic, non-relativistic and decaying mediator



# The out-of-equilibrium decay of a dark mediator.

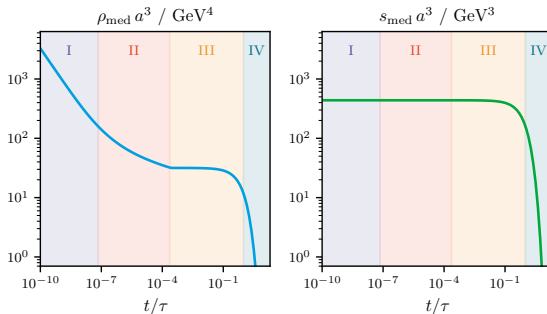
Number-changing processes of the mediator lead to a “cannibalistic” phase with  $\mu_{\text{med}} = 0$ . Therefore, the unique function  $\rho_{\text{med}}(s_{\text{med}})$  exists.

We found:

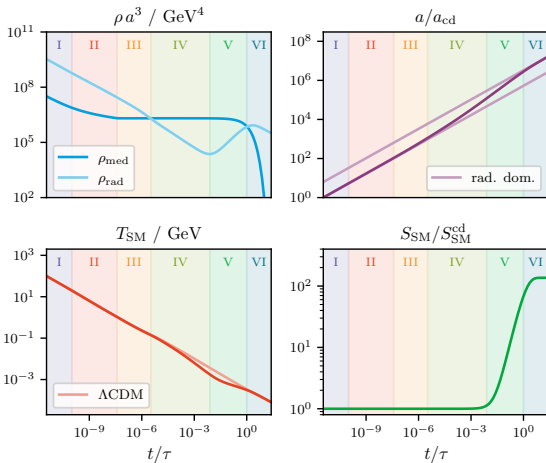
$$\zeta = \begin{cases} \frac{d \ln \rho_{\text{med}}}{d \ln s_{\text{med}}} & 3 \rightarrow 2 \text{ efficient} \\ 1 & 3 \rightarrow 2 \text{ inefficient} \end{cases}$$

During cannibalism,  $\zeta$  goes smoothly from  $4/3$  to  $1$ .

Four phases: Relativistic, cannibalistic, non-relativistic and decaying mediator



# The out-of-equilibrium decay of a dark mediator.



Energy densities  $\rho_i(t)$   $\rightsquigarrow$  Scale factor  $a(t)$   $\rightsquigarrow$  Temperatures  $T_{\text{SM}/\text{DS}}(t)$   $\rightsquigarrow$  Particle content  $\rightsquigarrow \rho_i(t)$   $\rightsquigarrow$  ...

## Six phases:

- I Relativistic mediator
- II Cannibalistic mediator
- III Non-relativistic mediator
- IV Early matter domination
- V Entropy injection
- VI Mediator decay

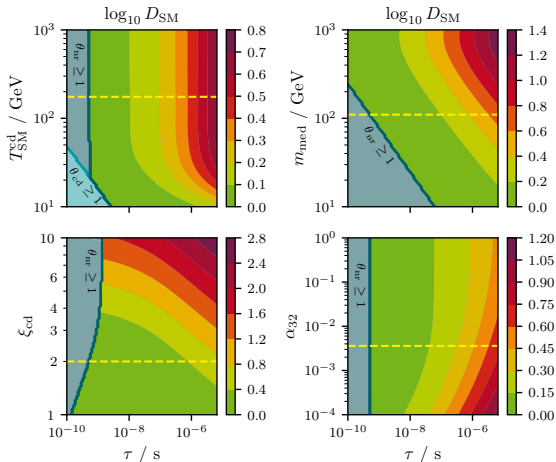
# The entropy injection into the SM bath.

Dilution factor: [1811.03608v3]

$$D_{\text{SM}} \equiv \frac{S_{\text{SM}}^{\text{after decay}}}{S_{\text{SM}}^{\text{before decay}}}$$

depends on:

- SM temperature  $T_{\text{SM}}^{\text{cd}}$  at chemical decoupling
- Mediator mass  $m_{\text{med}}$
- Temperature ratio  $\xi_{\text{cd}}$  at chemical decoupling
- Effective  $3 \rightarrow 2$  coupling  $\alpha_{32}$



## Parametrization of the GW signal.

Assuming strong<sup>1</sup> phase transitions, the GW spectrum can be parameterized by

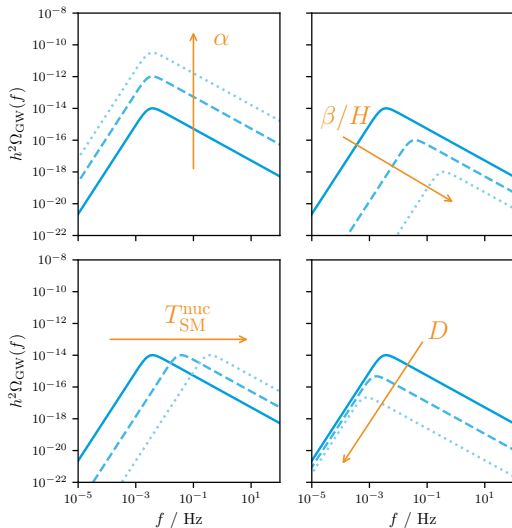
$$h^2 \Omega_{\text{GW}}(f) \simeq \frac{\mathcal{O}(10^{-6})}{D^{4/3}} \left( \frac{\alpha}{1+\alpha} \right)^2 \left( \frac{\beta}{H} \right)^{-2} \frac{3.8 (f/f_p)^{2.8}}{1 + 2.8 (f/f_p)^{3.8}}, \quad \text{where}$$

$$D \equiv \frac{g_{\text{eff},s}^{\text{SM,nuc}}}{g_{\text{eff},s}^{\text{tot,nuc}}} D_{\text{SM}} \quad \text{and} \quad f_p \simeq \frac{\mathcal{O}(10 \mu\text{Hz})}{D^{1/3}} \left( \frac{\beta}{H} \right) \left( \frac{T_{\text{SM}}^{\text{nuc}}}{100 \text{ GeV}} \right)$$

↪ GW spectrum fixed by the transition strength  $\alpha$ , the inverse time scale  $\beta/H$ , the nucleation temperature  $T_{\text{SM}}^{\text{n}}$  and the dilution factor  $D$

<sup>1</sup>This is only to get an intuition, the actually performed calculations are more involved

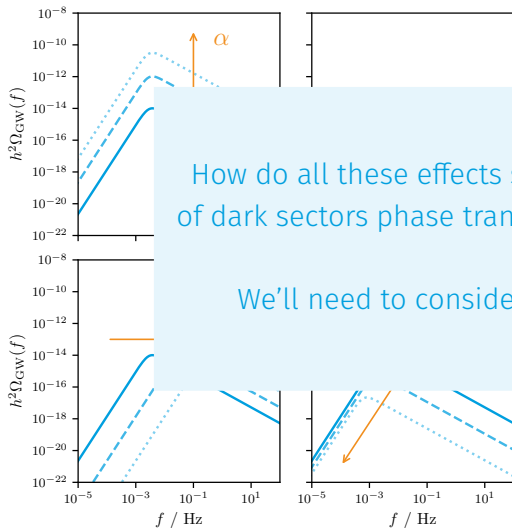
# Parametrization of the GW signal.



For observable signals:

- Strong transitions, high  $\alpha$
- Slow transitions, low  $\beta/H$
- Nucleation temperature  
 $T_{\text{SM}}^{\text{nuc}} \propto f_p \simeq f_{\text{exp}}$
- Little dilution, low  $D$

# Parametrization of the GW signal.



How do all these effects sum up and what kind of dark sectors phase transitions are observable?

We'll need to consider a specific model!

signals:

positions, high  $\alpha$

transitions, low  $\beta/H$

temperature

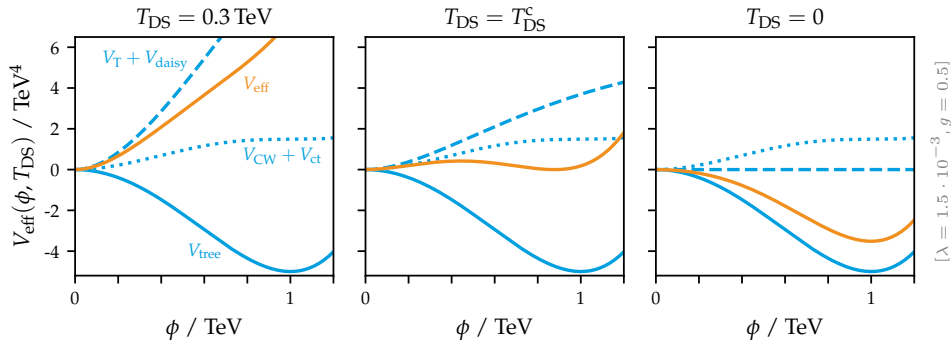
$f_{\text{exp}}$

on, low  $D$

## The dark photon model.

---

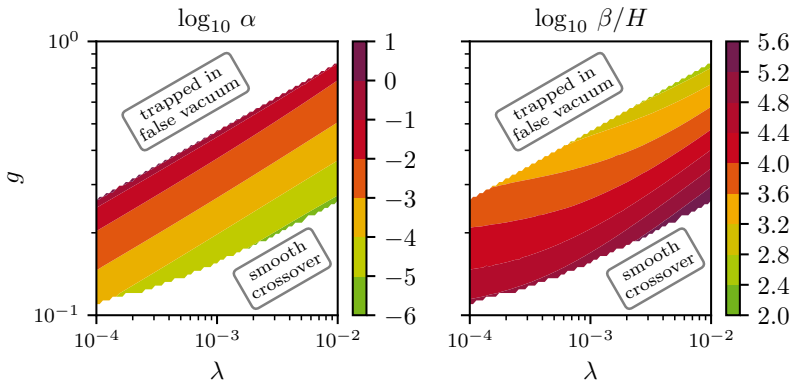
# The dark photon model.



Add a  $U(1)_D$  to the SM gauge groups. Its gauge boson, the “dark photon”, gets massive when a “dark Higgs” obtains  $\phi \neq 0$ . Effective potential controlled by the tree-level VEV  $v$ , dark Higgs quartic coupling  $\lambda$  and gauge coupling  $g$ .

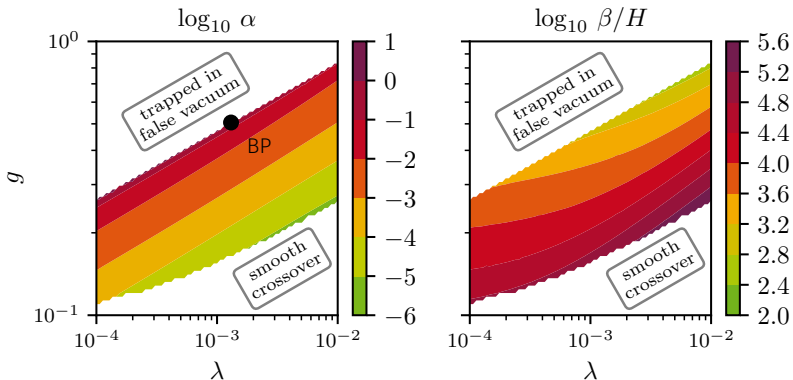
## Strength and time scale of the transition.

Analyze the phase structure and determine the strength  $\alpha$  and inverse time scale  $\beta/H$ . Vary quartic coupling  $\lambda$  and gauge coupling  $g$  to identify region of strong and slow transitions.

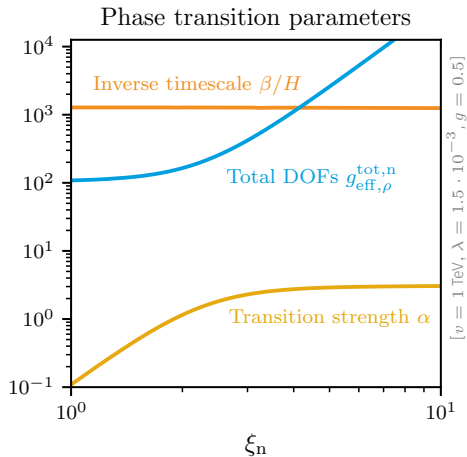


## Strength and time scale of the transition.

Analyze the phase structure and determine the strength  $\alpha$  and inverse time scale  $\beta/H$ . Vary quartic coupling  $\lambda$  and gauge coupling  $g$  to identify region of strong and slow transitions.

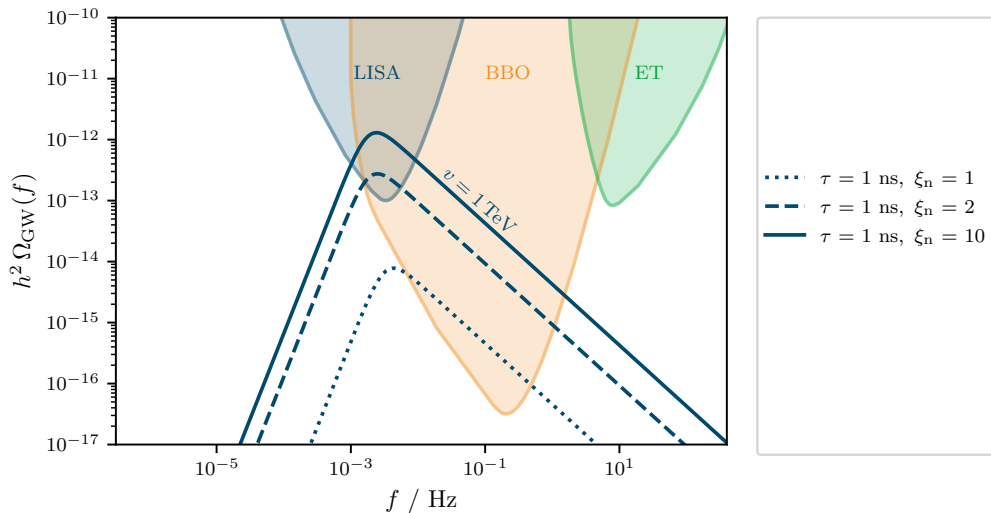


## The temperature ratio's impact on $\alpha$ and $\beta/H$ .

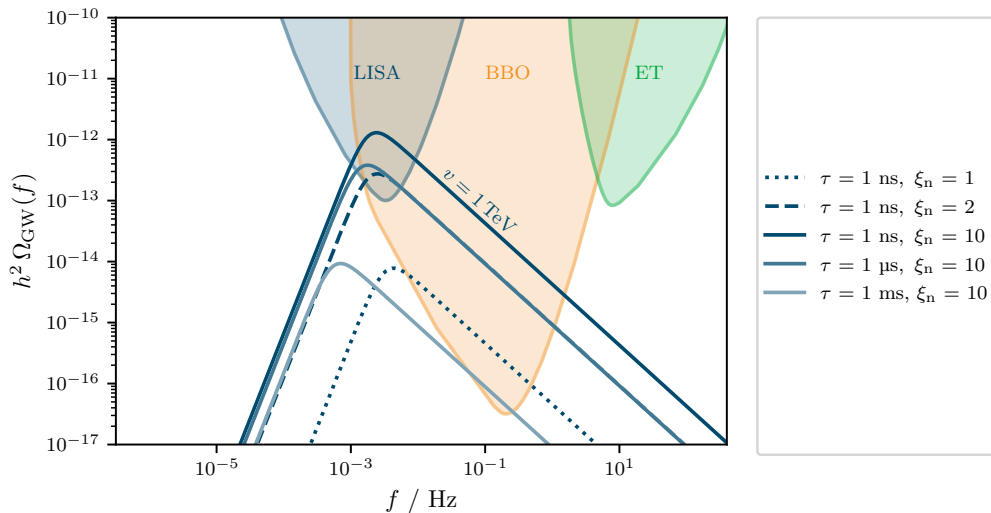


The transition strength  $\alpha$  increases  $\propto \xi_n^4$ , but only until the Universe is completely dominated by the dark sector. Then, the relative temperature difference becomes irrelevant. The inverse timescale is virtually independent of  $\xi_n$ .

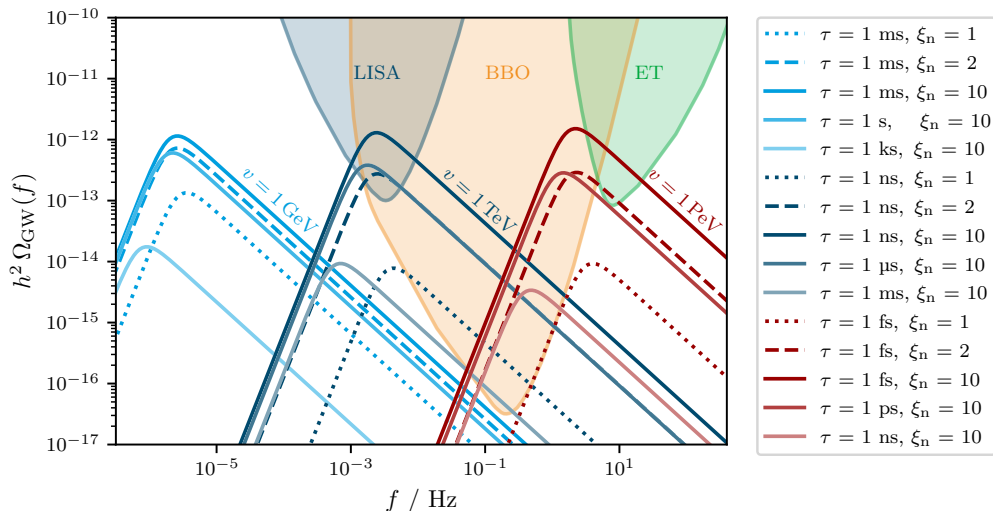
# The temperature ratio's impact on the GW signal.



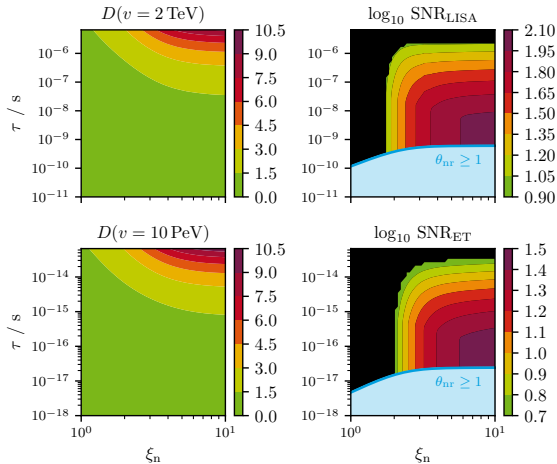
# The dark Higgs lifetime's impact on the GW signal.



# The vacuum expectation value's impact on the GW signal.



## Benchmark point analysis.

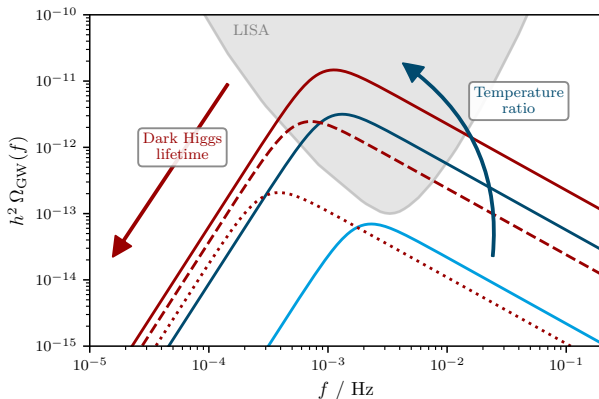


GWs observable by LISA and Einstein Telescope for  $\xi_n > 2$ , if dark sector is not too long-lived. Otherwise, signals are too diluted.

In blue region, the non-relativistic decay assumption breaks: Inverse decays become relevant, thermalizing the two baths.

# Summary.

- Hot dark sectors can produce strong first-order phase transitions
- Parts of the  $U(1)_D$  model parameter space will be testable by LISA and ET
- If the mediator species becomes too long-lived, its out-of-equilibrium decay will dilute the signal



## Conclusions.

---

## Conclusions and outlook.

- **Hot dark sector phase transitions** are experimentally testable!
- **Dilution** of GWs can be an important issue when dealing with dark sectors.
- **Our code** for model parameter scans, effective potentials, dilution factors, signal-to-noise ratios, etc. is available on github.
- **Bubble wall effects**  $\rightsquigarrow$  further work is necessary.
- **DM candidate** could easily be added to the model...
- **IPTA** [2201.03980] just observed something that looks as if it could be a dark sector phase transition at BBN temperatures... ?!

**Thank you very  
much for your  
attention!**

Please feel free to ask me  
about anything, if you have  
questions.



**Backup slides.**

---

## First-order phase transitions in thermal field theory.

To demonstrate construction of  $V_{\text{eff}}(\phi, T)$ , take the toy-model Lagrangian...

$$\mathcal{L} = \frac{1}{2} (\partial_\mu \phi) (\partial^\mu \phi) - V_{\text{tree}}(\phi)$$

$$\text{with } V_{\text{tree}}(\phi) = -\frac{1}{2}\mu^2\phi^2 + \frac{\lambda}{4}\phi^4$$

... and consider all 1-loop 1-PI graphs:

$$V_{\text{eff},\Phi}^{1\text{-loop}}(\phi) = \left[ \phi^2 \text{ (circle with 1 vertex) } + \phi^4 \text{ (circle with 2 vertices) } + \phi^6 \text{ (circle with 3 vertices) } + \dots \right]_{p=0}$$

## First-order phase transitions in thermal field theory.

And calculate 1-loop effective potential with  $m^2(\phi) = \partial_\phi^2 V_{\text{tree}}(\phi) = -\mu^2 + 3\lambda\phi^2$

$$\begin{aligned} V_{\text{eff}}(\phi, T) &= \frac{1}{2} \int \frac{d^4 k_E}{(2\pi)^4} \log [k_E^2 + m^2(\phi)] && \text{with } k_E^0 \text{ being } \frac{2\pi}{T}\text{-periodic} \\ &= \frac{T}{2} \sum_n \int_{\mathbf{k}} \log \left[ \left( \frac{2\pi n}{T} \right)^2 + E_k^2 \right] && \text{with } E_k = \sqrt{k^2 + m^2(\phi)} \\ &= \int_{\mathbf{k}} \left[ \frac{E_k}{2} + T \log \left\{ 1 - e^{-E_k/T} \right\} \right] \\ &= V_{\text{CW}}(\phi) + V_{\text{T}}(\phi, T) \end{aligned}$$

**Interpretation:**  $V_{\text{tree}}$  is the classical energy density contained in a background field  $\phi$ ,  $V_{\text{CW}}(+V_{\text{T}})$  is the vacuum energy density of a quantum field living in this background, which is completely analogous to the zero-point energy of a harmonic oscillator (in a thermal bath)

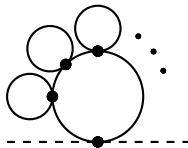
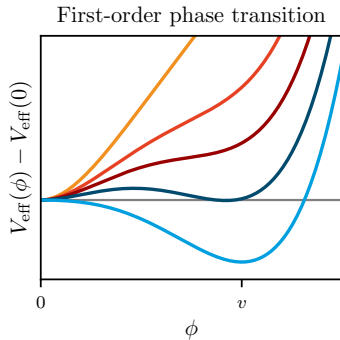
# First-order phase transitions in thermal field theory.

$$\begin{aligned} V_T &= \int_{\mathbf{k}} T \log \left\{ 1 - e^{-E_k/T} \right\} \\ &= -\frac{\pi^2 T^4}{90} + \frac{T^2 m^2(\phi)}{24} - \frac{T m^3(\phi)}{12\pi} + \dots \end{aligned}$$

However, around  $T_c$ ,  $V_{\text{eff}}$  is dominated by  $> 1$ -loop effects. “Daisies” dominate:

$$V_{\text{daisy}} = -\frac{T}{12\pi} \left[ (m^2(\phi) + \Pi(T))^{3/2} - m^3(\phi) \right]$$

And cancel the potential barrier in  $V_{\text{eff}}$ . But: Transversal gauge boson component doesn't acquire  $\Pi(T)$ .  $\rightsquigarrow$  Gauge bosons can save potential barrier and thus FOPTs.



# First-order phase transitions in thermal field theory.

## Summary:

$$V_{\text{eff}}^{1\text{-loop}}(\phi, T) = V_{\text{tree}}(\phi) + V_{\text{CW}}(\phi) + V_{\text{ct}}(\phi) + V_{\text{T}}(\phi, T) + V_{\text{daisy}}(\phi, T)$$

Coleman-Weinberg  
potential and its  
counter-terms

1-loop thermal  
corrections

Daisy corrections,  
dominate at  $T_c$

## How to get a thermal FOPT?

- Need scalar charged under gauge group with massive gauge bosons
- Dominant  $V_{\text{tree}} + V_{\text{CW}}$  contributions can always destroy potential barrier, though  $\rightsquigarrow$  as in SM with too high  $m_h$  forbidding FOPT

## First-order phase transitions in thermal field theory.

$$V_{\text{eff}}^{1\text{-loop}}(\phi, T) = V_{\text{tree}} + V_{\text{CW}} + V_{\text{ct}} + V_T + V_{\text{daisy}}$$

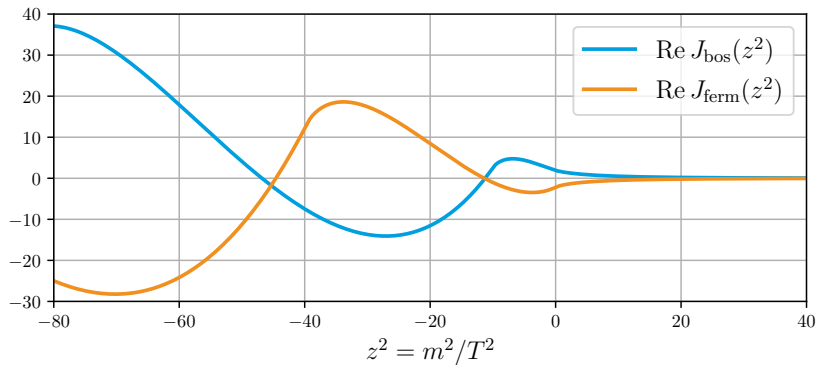
has the individual contributions

$$V_{\text{CW}}(\phi) = \sum_x \eta_x n_x \frac{m_x^4(\phi)}{64 \pi^2} \left[ \ln \frac{m_x^2(\phi)}{\Lambda^2} - C_a \right],$$

$$V_T(\phi, T) = \frac{T^4}{2 \pi^2} \sum_x \eta_x n_x J_{\eta_x} \left( \frac{m_x^2(\phi)}{T^2} \right),$$

$$V_{\text{daisy}}(\phi, T) = -\frac{T}{12 \pi} \sum_b n_b^{\perp} \left[ (m^2(\phi) + \Pi(T))_b^{3/2} - (m^2(\phi))_b^{3/2} \right]$$

# Thermal functions.



## Bubble expansion.

Euclidean action of scalar field

$$S[\phi] = \int d^4x_E \left[ \frac{1}{2} \left( \frac{\partial \phi}{\partial \tau} \right)^2 + \frac{(\nabla \phi)^2}{2} + V_{\text{eff}}(\phi) \right]$$

Minimizing for O(4)-case gives

$$\frac{d^2 \phi}{d\rho^2} + \frac{3}{\rho} \frac{d\phi}{d\rho} = V'_{\text{eff}}(\phi)$$

At finite  $T$  and in real space:

$$\frac{d^2 \phi}{dr^2} + \frac{2}{r} \frac{d\phi}{dr} = V'_{\text{eff}}(\phi, T)$$

Can be solved by overshoot-undershoot method

## Bubble formation and thermal tunneling.

Nucleation rate:  $\Gamma = \mathcal{A}e^{-S_4}$  with

$$S_4 = \int \frac{1}{2} \left( \frac{d\phi}{d\tau} \right)^2 + \frac{1}{2} (\nabla\phi)^2 + V_{\text{eff}}(\phi) d^4x_E$$

and  $\mathcal{A} \sim T^4$ . Extremalization yields KG equation with classical potential source:

$$\frac{d^2\phi}{d\tau^2} + \Delta\phi = \frac{dV_{\text{eff}}}{d\phi}$$

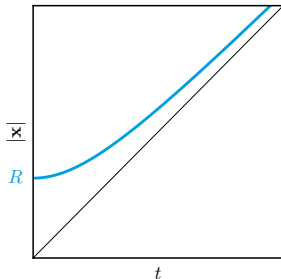
with b.c.  $\phi(\rho \rightarrow \infty) \rightarrow 0$  and

$\phi'(\rho = 0) = 0$  where  $\rho \equiv \sqrt{\tau^2 + |\mathbf{x}|^2}$ .

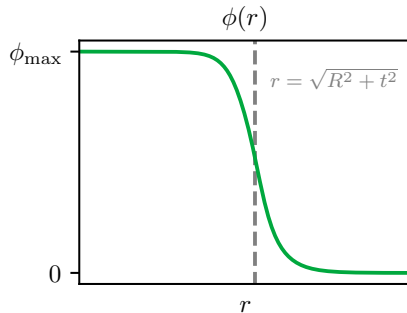
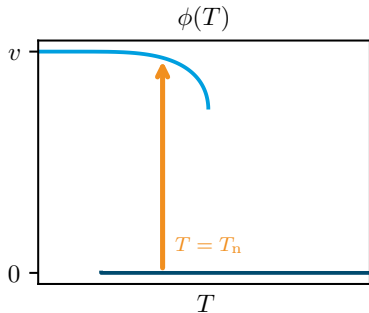
Solutions typically  $O(4)$  symmetric:

$$\frac{d^2\phi}{d\rho^2} + \frac{3}{\rho} \frac{d\phi}{d\rho} = \frac{dV_{\text{eff}}}{d\phi}$$

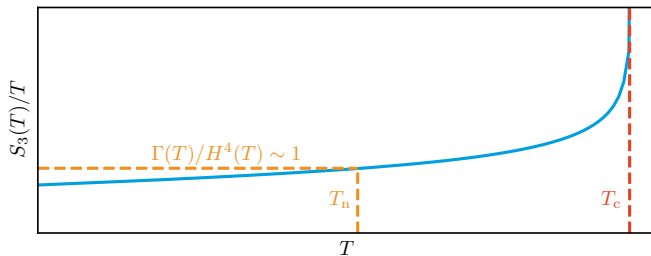
In 3-space:  $r = |\mathbf{x}| = \sqrt{\rho^2 - c^2t^2} \rightsquigarrow$   
Nucleation and expansion with  $v \rightarrow c$



# Temperature dependence of potential minima and bubble profile.



## Nucleation criterion.



The nucleation condition  $\Gamma(T_n) H^{-4}(T_n) = 1$  gives

$$\left. \frac{S_3(T)}{T} \right|_{T=T_n} \sim 146 - 2 \ln \left( \frac{g_{\text{eff},\rho}^{\text{tot}}(T_n)}{100} \right) - 4 \ln \left( \frac{T_n}{100 \text{ GeV}} \right)$$

Can be solved by repeated evaluation of  $S_3/T$  and subsequent minimization.

## GW parameter calculation.

Radiation energy density at nucleation

$$\rho_R = \frac{\pi^2}{30} \left( g_{\text{eff},\rho}^{\text{SM},n} + g_{\text{eff},\rho}^{\text{DS},n} \xi^4 \right) (T_{\text{SM}}^n)^4$$

Transition strength

$$\alpha^{(\text{DS})} = \frac{1}{\rho_R^{(\text{DS})}} \left( -\Delta V + \frac{1}{4} T_{\text{DS}}^n \left. \frac{\partial \Delta V}{\partial T} \right|_{T_{\text{DS}}^n} \right)$$

Inverse time scale

$$\frac{\beta}{H} = T_{\text{DS}}^n \left. \frac{dS_E(T)}{dT} \right|_{T_{\text{DS}}^n}$$

Critical transition strength for runaway bubbles ( $\alpha^{\text{DS}} > \alpha_{\infty}^{\text{DS}}$ )

$$\alpha_{\infty}^{\text{DS}} = \frac{(T_{\text{DS}}^n)^2}{\rho_R^{\text{DS}}} \left( \sum_{i=\text{bos}} n_i \frac{\Delta m_i^2}{24} + \sum_{i=\text{fer}} n_i \frac{\Delta m_i^2}{48} \right)$$

$$\Omega_{\text{GW}}(f) = \frac{1}{\rho_c} \frac{d\rho_{\text{GW}}(f)}{d \log f} \simeq \sum \mathcal{N} \Delta \left( \frac{\kappa \alpha}{1 + \alpha} \right)^p \left( \frac{H}{\beta} \right)^q s(f)$$

	Scalar field $\Omega_\phi$	Sound waves $\Omega_{\text{SW}}$	Turbulence $\Omega_{\text{turb}}$
$\mathcal{N}$	1	$1.59 \cdot 10^{-1}$	$2.01 \cdot 10^1$
$\kappa$	$\kappa_\phi$	$\kappa_{\text{SW}}$	$\varepsilon_{\text{turb}} \kappa_{\text{SW}}$
$p$	2	2	$\frac{3}{2}$
$q$	2	1	1
$\Delta$	$\frac{0.11 v_w^3}{0.42 + v_w^2}$	$v_w$	$v_w$
$f_p$	$\frac{0.62 \beta}{1.8 - 0.1 v_w + v_w^2}$	$\frac{2\beta}{\sqrt{3} v_w}$	$\frac{3.5\beta}{2 v_w}$
$s(f)$	$\frac{3.8(f/f_p)^{2.8}}{1 + 2.8(f/f_p)^{3.8}}$	$(f/f_p)^3 \left( \frac{7}{4 + 3(f/f_p)^2} \right)^{7/2}$	$\frac{(f/f_p)^3}{(1 + f/f_p)^{11/3} [1 + 8\pi(f/H)]}$

## Redshift and dilution of the GW background.

After its emission, the GW signal gets red-shifted:

$$h^2 \Omega_{\text{GW}}(f) = \mathcal{R}h^2 \Omega_{\text{GW}}^n \left( \frac{a_0}{a_n} f \right)$$

Energy density:

$$\mathcal{R}h^2 \simeq \frac{2.4 \cdot 10^{-5}}{D_{\text{SM}}^{4/3}} \left( \frac{g_{\text{eff},s}^{\text{SM},0}}{g_{\text{eff},s}^{\text{SM},n}} \right)^{4/3} \frac{g_{\text{eff},\rho}^{\text{tot},n}}{2}$$

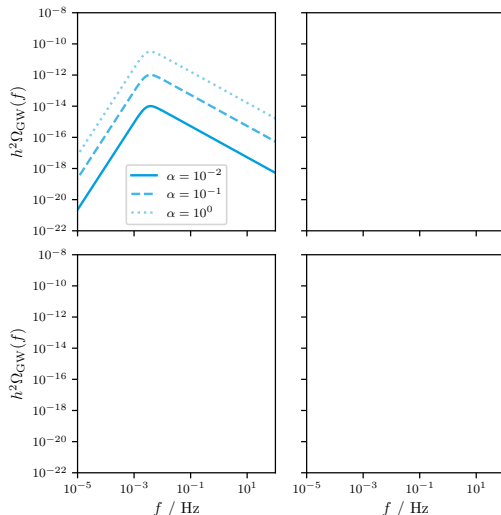
Frequency:

$$\frac{a_0}{a_n} = D_{\text{SM}}^{1/3} \left( \frac{g_{\text{eff},s}^{\text{SM},n}}{g_{\text{eff},s}^{\text{SM},0}} \right)^{1/3} \frac{T_{\text{SM}}^n}{T_{\text{SM}}^0}$$

## Transition strength:

$$\alpha = \frac{\Delta\theta}{\rho_{\text{rad}}^n}$$

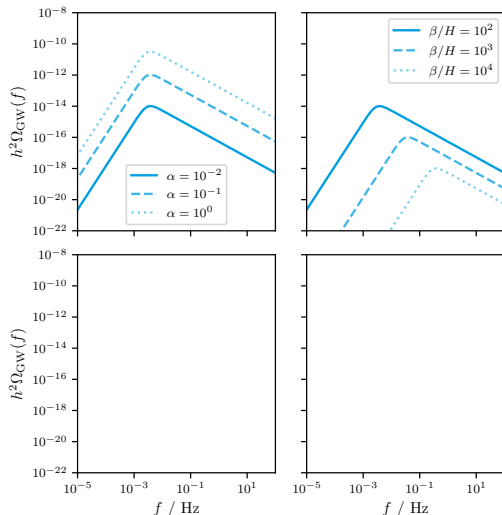
relates the latent heat (trace of the energy momentum tensor between the two phases)  $\Delta\theta$  of the transition with the energy density  $\rho_{\text{rad}}^n$  of the surrounding heat bath. For fixed  $T_{\text{DS}}^n$ :  $\rho_{\text{rad}}^n \propto \xi_n^{-4}$ . The transition strength thus grows  $\propto \xi_n^4$ .



# Parametrization of the GW signal.

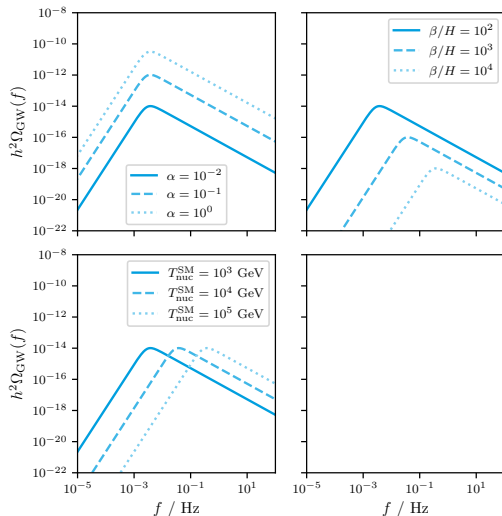
## Inverse time scale:

The computation of  $\beta/H$  is complicated, but shows no relevant dependence of the temperature ratio between the sectors. Larger  $\beta/H$  indicate fast transitions. In that case, many small bubbles collide, resulting in weak signals at high frequencies.



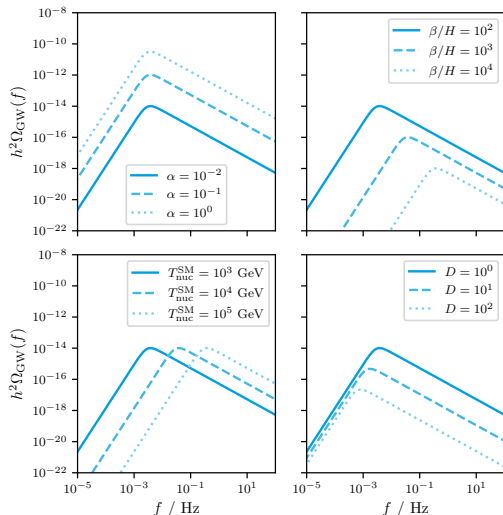
## Nucleation temperature:

Keeping  $T_{\text{DS}}^{\text{n}}$  fixed, a larger temperature ratio  $\xi_{\text{n}}$  at nucleation leads to a lower  $T_{\text{SM}}^{\text{n}}$ . This corresponds to lower peak frequencies.

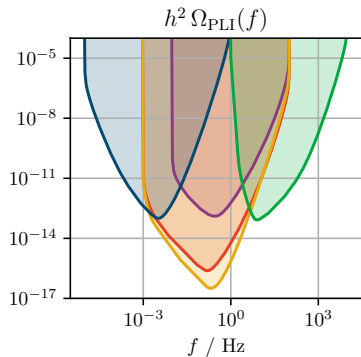
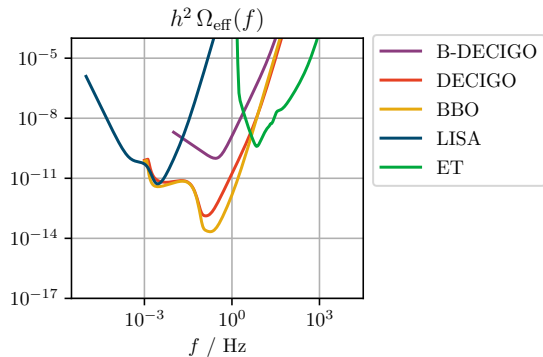


## Dilution:

The redshift to lower frequencies and signals strengths increases with the dilution factor.  $D$  grows with the temperature ratio  $\xi_n$ , as more energy is injected into the SM bath from the dark sector. Unlike  $D_{SM}$ ,  $D$  saturates for high temperature ratios.



# Experimental sensitivities.



## Effective degrees of freedom.

$$g_{\text{eff},\rho}^x(T_x) \equiv \frac{\rho_x(T_x)}{\rho_{\text{bos}}^{\text{rel}}(T_x)|_{g=1}} = g_x \frac{15}{\pi^4} \int_{z_x}^{\infty} du_x \frac{u_x^2 \sqrt{u_x^2 - z_x^2}}{e^{u_x} \pm 1},$$

$$g_{\text{eff},P}^x(T_x) \equiv \frac{P_x(T_x)}{P_{\text{bos}}^{\text{rel}}(T_x)|_{g=1}} = g_x \frac{15}{\pi^4} \int_{z_x}^{\infty} du_x \frac{(u_x^2 - z_x^2)^{3/2}}{e^{u_x} \pm 1},$$

$$g_{\text{eff},s}^x(T_x) = \frac{3 g_{\text{eff},\rho}^x(T_x) + g_{\text{eff},P}^x(T_x)}{4},$$

where  $u_x = \sqrt{m_x^2 + p^2}/T_x$  and  $z_x = m_x/T_x$ . Sum over all SM and DS species:

$$g_{\text{eff},\rho}^{\text{tot}} = g_{\text{eff},\rho}^{\text{SM}}(T_{\text{SM}}) + g_{\text{eff},\rho}^{\text{DS}}(T_{\text{SM}}) \xi^4(T_{\text{SM}})$$

$$g_{\text{eff},s}^{\text{tot}} = g_{\text{eff},s}^{\text{SM}}(T_{\text{SM}}) + g_{\text{eff},s}^{\text{DS}}(T_{\text{SM}}) \xi^3(T_{\text{SM}})$$

## Mediator cannibalism.

Conserved comoving mediator entropy  $s_{\text{med}} a^3 = \text{const}$  gives

$$\frac{d \ln s_{\text{med}}}{dt} = \frac{d \ln s_{\text{med}}}{d \ln \rho_{\text{med}}} \frac{\dot{\rho}_{\text{med}}}{\rho_{\text{med}}} = -3 H(t),$$

from which follows that

$$\dot{\rho}_{\text{med}} = -3 \frac{d \ln \rho_{\text{med}}}{d \ln s_{\text{med}}} H(t) \rho_{\text{med}}(t).$$

For  $\mu_{\text{med}} = 0$ , one can find function  $\rho_{\text{med}}(s_{\text{med}})$ , independent of particle species:

$$\frac{d \ln \rho_{\text{med}}}{d \ln s_{\text{med}}} = \frac{d \rho_{\text{med}}}{d s_{\text{med}}} \frac{s_{\text{med}}}{\rho_{\text{med}}} = \frac{d \bar{\rho}_{\text{med}}}{d \bar{s}_{\text{med}}} \frac{\bar{s}_{\text{med}}}{\bar{\rho}_{\text{med}}} = \frac{d \ln \bar{\rho}_{\text{med}}}{d \ln \bar{s}_{\text{med}}} = \frac{d \ln \bar{\rho}}{d \ln \bar{s}}$$

with  $\bar{s}_{\text{med}} \equiv 2 \pi^2 s_{\text{med}} / (g_{\text{med}} T_{\text{DS}}^3)$  and  $\bar{\rho}_{\text{med}} \equiv 2 \pi^2 \rho_{\text{med}} / (g_{\text{med}} T_{\text{DS}}^4)$ .

## Mediator cannibalism.

That yields

$$\dot{\rho}_{\text{med}} \simeq -3 \zeta H \rho_{\text{med}} - \rho_{\text{med}}/\tau$$

with

$$\zeta(t) = \begin{cases} \frac{d \ln \bar{\rho}}{d \ln \bar{s}}(\rho_{\text{med}}) & \text{for } \Gamma_{\text{nc}}(t) \geq H(t) \\ 4/3 & \text{for } \Gamma_{\text{nc}}(t) < H(t), \quad t < \tilde{t} \\ 1 & \text{for } \Gamma_{\text{nc}}(t) < H(t), \quad t \geq \tilde{t} \end{cases},$$

where  $\tilde{t} \simeq 7.0 t_{\text{cd}} (T_{\text{DS}}^{\text{cd}}/m_{\text{med}})^2$  denotes the time when the mediator gets non-relativistic. Number changing process rate is approximated by

$$\Gamma_{\text{nc}} \simeq \Gamma_{32} \simeq \langle \sigma_{32} v^2 \rangle n_{\text{med}}^2$$

The averaged cross section reads

$$\langle \sigma_{32} v^2 \rangle = \frac{25 \sqrt{5} \pi^2}{5184} \frac{\alpha_{32}^3}{m_{\text{med}}^5} + \mathcal{O} \left( \frac{T_{\text{DS}}}{m_{\text{med}}} \right).$$

where

$$(4 \pi \alpha_{32})^3 \equiv \left( \frac{\kappa_3}{m} \right)^2 \left[ \left( \frac{\kappa_3}{m} \right)^2 + 3 \kappa_4 \right]^2$$

for a potential  $V(\phi) = \frac{m^2}{2} \phi^2 + \frac{\kappa_3}{3!} \phi^3 + \frac{\kappa_4}{4!} \phi^4$ . In our model:  $\alpha_{32} = 2.3 \lambda$ .

## Coupled set of ODEs underlying the entropy injection.

$$\begin{aligned}\bar{a}' &= \frac{\bar{a}}{\theta_H} \sqrt{r + \frac{r_{\text{mat}}^{\text{cd}}}{\bar{a}^3} + \frac{r_{\text{rad}}^{\text{cd}}}{\bar{a}^4} \frac{\gamma}{\gamma_{\text{cd}}} \frac{\mathcal{S}}{\mathcal{G}^{1/3}}}, \\ \mathcal{S}' &= \frac{r \bar{a}^4}{r_{\text{rad}}^{\text{cd}}} \mathcal{G}^{1/3} \gamma_{\text{cd}}, \\ r' &= -r - 3 \frac{\bar{a}'}{\bar{a}} \zeta r, \\ \mathcal{G}' &= -\frac{3}{4} \frac{T_{\text{SM}}^{\text{cd}} \mathcal{G} \hat{\mathcal{G}}}{\mathcal{S}^{3/4} \bar{a}} \frac{4 \mathcal{S} \bar{a}' - \mathcal{S}' \bar{a}}{T_{\text{SM}}^{\text{cd}} \hat{\mathcal{G}} \mathcal{S}^{1/4} + 3 \mathcal{G}^{4/3} \bar{a}}, \\ \gamma' &= \hat{\gamma} T_{\text{SM}}^{\text{cd}} \frac{3 \mathcal{G} \bar{a} \mathcal{S}' - 12 \mathcal{G} \bar{a}' \mathcal{S} - 4 \mathcal{G}' \bar{a} \mathcal{S}}{12 \mathcal{G}^{4/3} \mathcal{S}^{3/4} \bar{a}^2}.\end{aligned}$$

with initial condition  $\bar{a}_{\text{cd}} = \mathcal{S}_{\text{cd}} = r_{\text{cd}} = \mathcal{G}_{\text{cd}} = 1$  and  $\gamma_{\text{cd}}$ .

- Normalized scale factor  $\bar{a} = a/a_{\text{cd}}$
- Characteristic time scale  $\theta_H = \sqrt{3 m_{\text{Pl}}^2 \rho_{\text{med}}^{\text{cd}}/\tau^2}$
- Normalized mediator energy density  
 $r = \rho_{\text{med}}/\rho_{\text{med}}^{\text{cd}}$
- Normalized initial DM density  $r_{\text{mat}}^{\text{cd}} = \rho_{\text{DM}}^{\text{cd}}/\rho_{\text{med}}^{\text{cd}}$
- Normalized initial radiation energy density  
 $r_{\text{rad}}^{\text{cd}} = \rho_{\text{rad}}^{\text{cd}}/\rho_{\text{med}}^{\text{cd}}$
- Normalized DOFs  $\gamma = g_{\text{eff},\rho}^{\text{SM}}/g_{\text{eff},s}^{\text{SM}}$
- Normalized DOFs  $\mathcal{G} = g_{\text{eff},s}^{\text{SM}}/g_{\text{eff},s}^{\text{SM,cd}}$
- Normalized SM entropy  $\mathcal{S} = \left(S_{\text{SM}}/S_{\text{SM}}^{\text{cd}}\right)^{4/3}$

## The $U(1)_D$ model in detail.

Lagrangian:

$$\mathcal{L} \supset |D_\mu \Phi|^2 + |D_\mu H|^2 - \frac{1}{4} B'_{\mu\nu} B'^{\mu\nu} - \frac{\epsilon}{2} B'_{\mu\nu} B^{\mu\nu} - V(\Phi, H) ,$$

$$D_\mu \Phi = (\partial_\mu + i g B'_\mu) \Phi ,$$

$$V_{\text{tree}}(\Phi, H) = -\mu^2 \Phi^* \Phi + \lambda (\Phi^* \Phi)^2 - \mu_H^2 H^\dagger H + \lambda_H (H^\dagger H)^2 + \lambda_p (\Phi^* \Phi) (H^\dagger H) .$$

Mass spectrum:

$$m_{(h, \phi)}^2(h, \phi) = \begin{pmatrix} -\mu_H^2 + 3 \lambda_H h^2 + \frac{\lambda_p}{2} \phi^2 & \lambda_p h \phi \\ \lambda_p h \phi & -\mu^2 + 3 \lambda \phi^2 + \frac{\lambda_p}{2} h^2 \end{pmatrix} ,$$

$$m_{G^0, G^+}^2(h, \phi) = -\mu_H^2 + \lambda_H h^2 + \frac{\lambda_p}{2} \phi^2 ,$$

$$m_\varphi^2(h, \phi) = -\mu^2 + \lambda \phi^2 + \frac{\lambda_p}{2} h^2 .$$

## The $U(1)_D$ model in detail.

For  $\lambda_p, \epsilon \rightarrow 0$  and  $\mu^2 = \lambda v^2$ , the field-dependent dark Higgs and dark photon masses are given by

$$m_{\text{DP}} = g \phi \stackrel{T=0}{=} g v ,$$

$$m_{\text{DH}} = \sqrt{2\lambda} \phi \stackrel{T=0}{=} \sqrt{2\lambda} v .$$

The corresponding Debye masses are

$$\Pi_{\Phi}(T_{\text{DS}}) = \left( \frac{\lambda}{3} + \frac{g^2}{4} \right) T_{\text{DS}}^2 ,$$

$$\Pi_{A'}^L(T_{\text{DS}}) = \frac{g^2}{3} T_{\text{DS}}^2 .$$

- Quartic dark Higgs coupling:  $\lambda$
- $U(1)_D$  gauge coupling:  $g$
- Dark Higgs lifetime:  $\tau$
- Dark Higgs VEV:  $v = \frac{\mu}{\sqrt{\lambda}}$
- Temperature ratio:  $\xi_n = \left. \frac{T_{\text{DS}}}{T_{\text{SM}}} \right|_n$

## Signal-to-noise ratios for LISA and the ET.

Compute the overlap of the signals  $h^2 \Omega_{\text{GW}}(f)$  and expected sensitivities  $h^2 \Omega_{\text{obs}}(f)$  and weight it with the duration of the observation  $t_{\text{obs}}$  to obtain a signal-to-noise measure:

$$\rho^2 = t_{\text{obs}} \int_{f_{\text{min}}}^{f_{\text{max}}} df \left[ \frac{h^2 \Omega_{\text{GW}}(f)}{h^2 \Omega_{\text{obs}}(f)} \right]^2$$

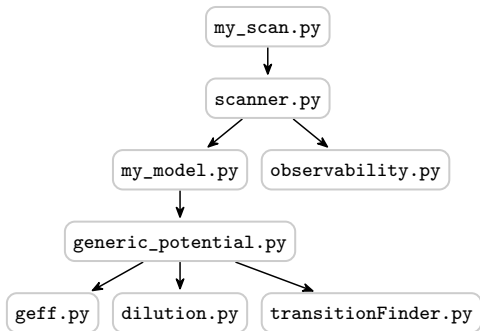
If  $\rho$  exceeds a certain threshold value for a given signal, the signal is observable.

To analyze the impact of  $\xi_n$  and  $\tau$  on the observability of the signals produced by our model, consider the benchmark points

Benchmark point	$\lambda$	$g$	$v$
LISA	$1.5 \cdot 10^{-3}$	0.5	2 TeV
ET	$1.5 \cdot 10^{-3}$	0.5	10 PeV

# Structure of TransitionListener.

Structure:



Example output:

